

Subradiance in dilute atomic ensembles excited by nonresonant radiation

Y. A. Fofanov¹ and I. M. Sokolov^{1,2}

¹Institute for Analytical Instrumentation, Russian Academy of Sciences, 190103, St.-Petersburg, Russia

² Peter the Great St. Petersburg Polytechnic University, 195251 St. Petersburg, Russia

R. Kaiser and W. Guerin

Université Côte d'Azur, CNRS, Institut de Physique de Nice, Valbonne, France

(Dated: July 9, 2022)

We numerically study the slow (subradiant) decay of the fluorescence of motionless atoms after a weak pulsed excitation. We show that, in the linear-optics regime and for an excitation detuned by several natural linewidths, the slow decay rate can be dominated by close pairs of atoms (dimers) forming superradiant and subradiant states. However, for large-enough resonant optical depth and at later time, the dynamics can also be dominated by radiation trapping due to classical multiple scattering. Signatures of this regime are found in the spatial distribution of excited atoms, which fulfills the prediction of the diffusion equation, in the polarization of the emitted light, which is depolarized at late time, and in the spectrum, which is mainly at the atomic resonance.

I. INTRODUCTION

Collective effects in light-atom interactions are at the focus of intense research, in particular for the potential applications to quantum optics and photonics [1]. In this context, subradiance, corresponding to the reduced spontaneous emission of some collective modes [2–4], received considerable attention, with several experimental demonstrations [5–8]. The long subradiant lifetimes may be used for storage and retrieval of quantum information [9–12] and other photonic devices, for instance single-atomic layer mirrors [8] and nanolasers [13].

In the framework of a coupled-dipole picture, in which the light degrees of freedom are traced out and atoms interact with each other through the dipole-dipole interaction, the system properties can be described with eigenmodes and complex eigenvalues [14, 15]. One can then classify the collective atomic states in two categories. The superradiant and subradiant modes have decay rates larger and smaller than the single atom one, respectively. Subradiance is thus a generic term for all long-lived modes. From another physical point of view, in which one would describe the electromagnetic field interacting with the atoms modeled as point-dipole scatterers, the long lifetime of light in the system can have several origins [16]: trapping due to refractive index boundaries or gradient [17, 18], radiation trapping due to multiple scattering [19], with eventually mesoscopic corrections such as recurrent scattering, weak and strong localization effects [20], etc.

In this article, we discuss the nature of subradiance in the following case: The system is driven with a weak-intensity laser (linear-optics regime), with a plane wave, the sample is 3D, statistically homogeneous, and dilute (the average interparticle distance is larger than the inverse of the wave number), atoms are motionless and located at random positions. Moreover the slow decay is studied after averaging over many realizations of the positional disorder. We show that, in this regime of parameters, there are two main contributions to the subra-

diant decay: recurrent scattering within diatomic clusters and radiation trapping. This is inferred from the computation, using the coupled-dipole model, of the temporal dynamics of the fluorescence, as done in many earlier works, but also using observables not studied so far in this context, such as the spatial distribution of atomic excitation, the spectrum of the fluorescence and its polarization. Our findings provide a better understanding of the physics of subradiance in dilute disordered systems.

The paper is organized as follows. In the next section we present the coupled-dipole model and the parameters we use. In section III we present our numerical results on the decay dynamics of the fluorescence, including spatial, spectral and polarization properties. Finally in section IV we discuss and conclude on the remaining open questions.

II. BASIC ASSUMPTIONS AND APPROACH

A. Coupled-dipole model

We consider an ensemble consisting of $N \gg 1$ identical atoms with a nondegenerate ground state of angular momentum $J_g = 0$. The excited states is $J_e = 1$. The lifetimes of all three of its Zeeman sublevels ($m = -1, 0, 1$) are the same and equal to $\tau_{\text{at}} = 1/\gamma$. We describe the evolution of the atomic states by the coupled-dipole (CD) model, which is traditional for this class of problems. This model was first proposed by Foldy [21], then discussed in detail by Lax [22]. Later a similar approach was used in the context of different types of collective effects such as multiple and recurrent scattering, collective spontaneous decay and Anderson localization of light [4, 5, 14, 15, 23–33].

In this work we use a version of the CD model formulated in the framework of the sequential quantum approach developed in [34]. Without repeating the derivation, let us note only its main features. We analyze the properties of a closed system consisting of all atoms and

an electromagnetic field, including a vacuum reservoir. We look for the wave function ψ of this system in the form of an expansion over the eigenfunctions ψ_l of the Hamiltonian of noninteracting atoms and light $\psi = \sum_l b_l \psi_l$. Considering the case of weak excitation and restricting ourselves to the states of the atomic-field system containing no more than one photon, for the amplitudes b_e of one-fold excited atomic states $\psi_e = |g \cdots e \cdots g\rangle$, we have the following set of equations:

$$\frac{\partial b_e}{\partial t} = \left(i\delta_e - \frac{\gamma}{2} \right) b_e - \frac{i\Omega_e}{2} + \frac{i\gamma}{2} \sum_{e' \neq e} V_{ee'} b_{e'}. \quad (1)$$

Here, the index e denotes the number of the atom that is excited in the state $\psi_e = |g \cdots e \cdots g\rangle$, as well as the specific populated Zeeman sublevel.

The first term of the right-hand side of Eq. (1) describes the natural evolution of independent atomic dipoles. The second one corresponds to the driving by the external laser field. The Rabi frequency of the field at the point where atom e is located is Ω_e . Its detuning δ_e may be different for different transitions $g \leftrightarrow e$. The last term in Eq. (1) describes the dipole-dipole interaction and is responsible for all collective effects. It reads

$$V_{ee'} = -\frac{2}{\gamma} \sum_{\mu, \nu} \mathbf{d}_{eg}^\mu \mathbf{d}_{ge'}^\nu \frac{e^{ikr_{ij}}}{\hbar r_{ij}^3} \times \left\{ \delta_{\mu\nu} [1 - ikr_{ij} - (kr_{ij})^2] - \frac{\mathbf{r}_{ij}^\mu \mathbf{r}_{ij}^\nu}{r_{ij}^2} [3 - 3ikr_{ij} - (kr_{ij})^2] \right\}. \quad (2)$$

Here we assume that in the states e and e' atoms i and j are excited; $\mathbf{r}_{ij} = \mathbf{r}_i - \mathbf{r}_j$, $r_{ij} = |\mathbf{r}_i - \mathbf{r}_j|$; \mathbf{d}_{eg} is the matrix element of the dipole moment operator for the transition $g \rightarrow e$, and $k = \omega_0/c$ is the wavenumber associated to the transition, c the vacuum speed of light. The superscripts μ or ν denote projections of vectors on one of the axes $\mu, \nu = x, y, z$ of the reference frame.

The system (1) is solved numerically many times for various random spatial configurations of motionless atoms. From the computed values of $b_e(t)$, we can find the amplitudes of all other states that determine the wave function ψ of the joint atom-field system for a given configuration (for more detail see [34]). Knowing the wave function, we can determine all the properties of both the atomic subsystem and the radiation. For example, the intensity $I_\alpha(\Omega, t)$ of the polarization component of the light α , emitted by the cloud in a unit solid angle around an arbitrary direction given by the wave vector $\mathbf{k}(\Omega = \theta, \varphi)$, can be defined as follows [35]:

$$I_\alpha(\Omega, t) = \frac{c}{4\pi} \left| k^2 \sum_{i,m} (\mathbf{u}_\alpha^* \mathbf{d}_{ge}) \beta_e(t) \exp(-i\mathbf{k}\mathbf{r}_i) \right|^2. \quad (3)$$

Here \mathbf{u}_α is the unit polarization vector of the secondary radiation.

It is also possible to compute the radiated field $E_\alpha(\mathbf{r}, t)$ and take the squared modulus of its Fourier transform to get the spectrum of the fluorescence, in a given time window.

The computed observables are averaged by the Monte Carlo method over the random spatial distribution of atoms.

B. Parameters of the system

Calculations of the dynamics of fluorescence by the CD method can be carried out for an arbitrary inhomogeneous spatial distribution of atoms and for an arbitrary shape of the atomic cloud. In our case, the shape and distribution have only a quantitative influence, without changing the basic physics of the investigated effects. For this reason, in this work, we consider the geometrically simplest case of an average homogeneous ensemble of cubic shape. Although the sharp boundaries might create specific modes [17], this choice simplifies the analysis of the spatial distribution of excited atoms and its change with time. In addition, for a simple geometry with relatively sharp boundaries of the atomic ensemble and a uniform spatial distribution of atoms (in average), it is possible to compare the numerical results with the predictions of the diffusion theory of radiative transfer.

The density of atoms n in all calculations will be the same: $n = 0.01k^3$. Such a choice makes it possible to approximately simulate the dilute atomic ensembles that are dealt with in experiments. The excitation pulse is assumed to be rectangular, its carrier frequency ω is detuned from the transition frequency ω_0 of a free atom by a detuning $\delta = \omega - \omega_0$. The pulse duration is $\gamma T = 2000$, which makes it possible to excite atoms in a rather narrow spectral range near the laser frequency. The laser radiation is assumed to be circularly polarized.

At a fixed density of atoms, a series of calculations was performed for different sizes L of the atomic cloud and different detunings δ . When choosing the detunings, we limited ourselves to the case when the optical thickness of the medium at the excitation frequency does not exceed a value on the order of 1. For the considered density and for the largest cloud containing 10^4 atoms, it corresponds to $|\delta| \geq 2\gamma$. We also note that all the following results were obtained for negative detunings. We have checked that the qualitative conclusions remain valid even with positive detunings, with only slight quantitative changes.

III. RESULTS

A. Decay dynamics of the fluorescence intensity

First, we compute the total relative intensity $I(t)/I(0)$ of the fluorescence emitted in all directions and in all po-

larization channels. From that we compute the ‘instant trapping time’ $\tau(t)$, which is defined as the inverse of the instantaneous decay rate $\tau(t) = 1/\Gamma(t)$, where

$$\Gamma(t) = -d \ln(I(t))/dt. \quad (4)$$

It was found in previous studies on subradiance [5, 36] that the subradiant lifetime depends linearly on the resonant optical thickness $b_0 = n\sigma_0 L$ ($\sigma_0 = 6\pi/k^2$ is the resonance cross section of a single atom). Here, our calculations reveal a more complex behavior of the fluorescence dynamics and its instantaneous decay. For each detuning δ there is a certain characteristic size of the atomic ensemble L (or b_0), below which $I(t)/I(0)$ and $\tau(t)$ practically do not change with b_0 .

Fig. 1 demonstrates such a behavior for $\delta = -4\gamma$. The curves correspond to different sizes (labeled in the figure), corresponding to different b_0 from 1.1 to 13.2 and different atom numbers from $N = 2$ to $N = 3430$. Up to $kL = 70$ the curves $I(t)/I(0)$ and $\tau(t)$ for different sizes of the ensemble practically do not differ within the accuracy of the calculations. In a significant range of time, they also do not differ much from the curves obtained for a diatomic ensemble $N = 2$ (green solid line, $kL = 5.848$). In the range from $\gamma t \simeq 50$ to $\gamma t \simeq 150$, the relative difference for the relative intensity between the results for the smallest number of atoms and the largest one does not exceed 5%. In the middle of this time interval, it is significantly less, on the order of 1%.

We attribute this behavior to the impact of pairs of close atoms (dimers) building subradiant states. To support this interpretation, we compute the level shifts Δ_r and the decay rate Γ_r of the excited states of such diatomic quasimolecules, which depend on the distance r between the atoms. For the considered case of $J_e = 1$, there are six states, two pairs of which are identical, with

$$\begin{aligned} \frac{\Delta_r}{\gamma} &= \frac{3\epsilon}{4} \left(-\frac{p \cos(kr)}{kr} + q \left(\frac{\cos(kr)}{(kr)^3} + \frac{\sin(kr)}{(kr)^2} \right) \right), \\ \frac{\Gamma_r}{\gamma} &= 1 - \frac{3\epsilon}{2} \left(-\frac{p \sin(kr)}{kr} + q \left(\frac{\sin(kr)}{(kr)^3} - \frac{\cos(kr)}{(kr)^2} \right) \right), \end{aligned}$$

with $\epsilon = \pm 1$; $p_0 = 0$; $q_0 = -2$; $p_{\pm 1} = 1$; $q_{\pm 1} = 1$.

Among these states there are long-lived, subradiant states. The energy shift corresponding to the detuning $\Delta_r = -4\gamma$ is achieved at $kr \approx 0.549$. At such distance, the lifetime of the long-lived states are approximately equal to $1/\Gamma_r \approx 16.86\tau_{\text{at}}$. The horizontal line in the lower Fig. 1 corresponds to this value. Long excitation by monochromatic light with this detuning is most likely to excite diatomic clusters with this distance between atoms, while other collective states are off resonance. These clusters thus provide the main contribution to the fluorescence in a quite large time interval. At very late times, when these long-lived states have decayed, the main contribution to fluorescence come from longer-lived states and we observe an increase in the instant trapping time. Note that these pairs, whose influence on light transport in atomic gases has been first discussed in [37],

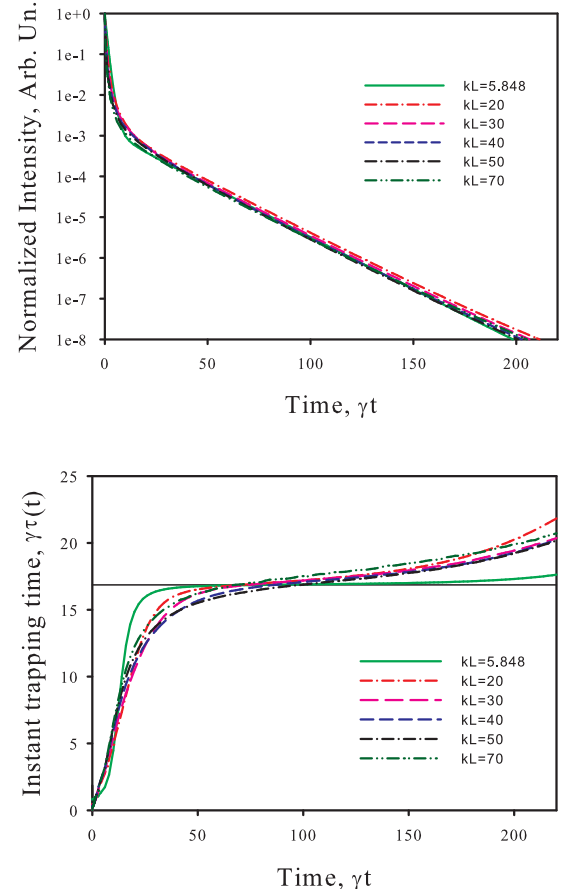


FIG. 1. Fluorescence dynamics of atomic ensembles of various sizes. The density of atoms is $n = 0.01k^3$, the duration of excitation is $\gamma T = 2000$, its detuning is $\delta = -4\gamma$. The number of realizations changes from 10^4 ($kL = 20$) to 5000 ($kL = 70$). The upper panel is the total normalized radiation intensity in all directions and polarizations $I(t)/I(0)$, the lower panel is the instant trapping time $\tau(t)$. The smallest size (green solid line) corresponds to $N = 2$ atoms (4×10^6 realizations in that case). The horizontal black solid line in the lower panel corresponds to the computed lifetime of subradiant dimers that are resonant with the excitation.

were voluntarily removed in Refs. [5, 36, 38] by drawing the random atomic positions with an exclusion volume.

With a further increase of b_0 , the situation changes, see Fig. 2. After some time, the decay dynamics of the fluorescence begins to depend on the size of the atomic ensemble. For the parameters under consideration, such changes are observed for $\gamma t \geq 50$. For the sizes $kL \geq 80$, one can clearly see an increase of $\tau(t)$, with a tendency towards stationary values, which depend on the size of the ensemble.

The difference in the behavior of the curves at long times in Fig. 1 and Fig. 2 shows that different mechanisms are at play. As discussed previously, for detuned excitation, moderate b_0 and moderate time delay, diatomic Dicke subradiance dominates. We argue in the following

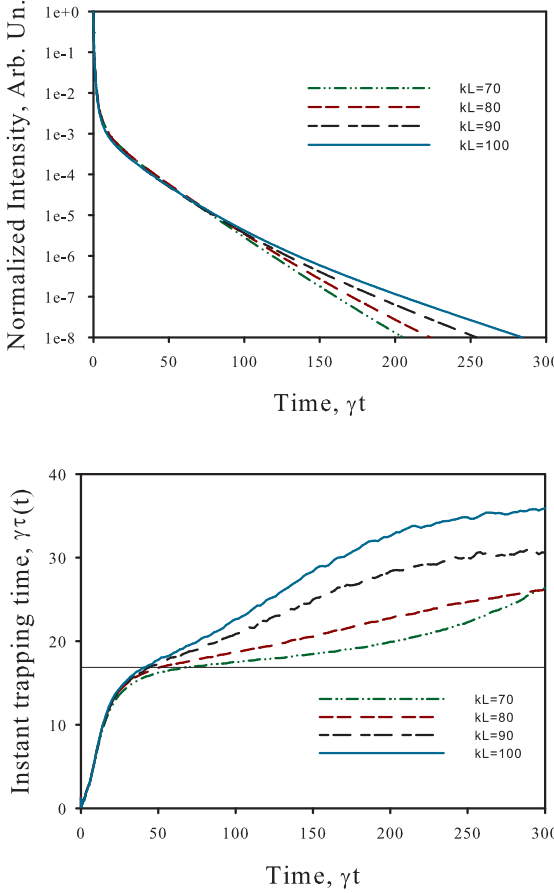


FIG. 2. Same as in Fig. 1 with larger sample sizes L . The number of realizations changes from 5000 ($kL = 70$) to 300 ($kL = 100$).

that, in the opposite regime of large b_0 and late time, slow diffusion of light due to multiple scattering, or ‘radiation trapping’, is the main contribution to the slow decay of the fluorescence [19].

Radiation trapping can only occur when the photon mean free path is much shorter than the medium size, which is not the case for light detuned by several natural linewidths such that the incident field that we consider. However, even when the system is driven off resonance, some resonant light is always present during the decay dynamics. This can be understood, in a ‘photon picture’, by the fact that the switch-on and off of the driving field introduces some spectral broadening. Alternatively, in the coupled-dipole picture, the presence of resonant light during the decay is due to the fact that, after the driving field is switched off, the weakly-excited collective states decay at their own frequency, which is close to the natural atomic resonance. This generation of resonant light has been overlooked in previous papers discussing subradiance in dilute sample [4, 5, 38].

Radiation trapping introduces a new characteristic timescale, which is the lifetime of the longest diffusive

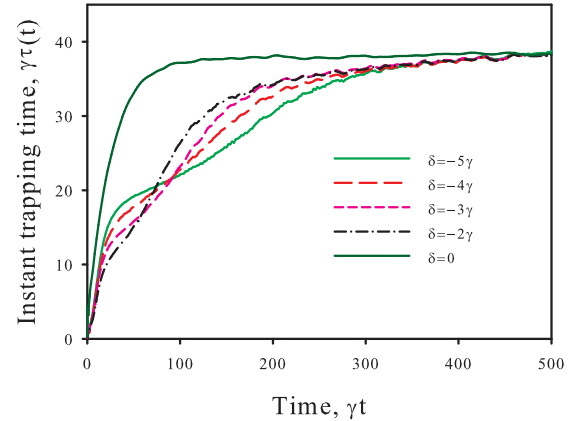


FIG. 3. Instant trapping time $\tau(t)$ for different detunings δ of the exciting radiation. The system size is $kL = 100$ ($b_0 \approx 19$) and the number of realizations is 300. At late time radiation trapping dominates while at intermediate time and at large detuning, the decay rate due to diatomic clusters is well visible.

mode,

$$\tau_{\text{diff}} = \frac{3b^2}{\alpha\pi^2}\tau_{\text{at}}, \quad (5)$$

where α depends on the shape of the atomic clouds [19]. For homogeneous (in average) cubic ensembles, $\alpha = 3$ [39]. This formula is only valid in the diffusive regime, i.e. when $b \gg 1$. Also, the optical depth b here slightly differs from b_0 by some addition b' ($b = b_0 + b'$) depending on the photon mean-free path. This difference is due to the extrapolation length for the boundary conditions of the radiative diffusion equation (see Fig. 4 and for more detail, see for example [20]).

It is possible to determine the parameters (size and detuning) for which radiation trapping begins to play a noticeable role by comparing this diffusive lifetime with the lifetime of long-lived states of diatomic quasimolecules $\tau_r = 1/\Gamma_r$, the transition frequency of which coincides with the frequency of the exciting pulse $\Delta_r = \delta$. These are the quasi-molecules that are efficiently excited. When $\tau_{\text{diff}} > \tau_r$, the main mechanism of subradiance should become radiation trapping after a certain time delay. Note, however, that after the decay of the slowest diffusion mode, the situation changes. Diatomic subradiance due to off-resonantly excited pairs, with smaller r , becomes dominant again. But for large optical depths, this occurs at very late time after the end of the excitation, when the fluorescence signal becomes too small to be experimentally relevant.

The comparison between τ_{diff} and τ_r , and consequently the respective role of radiation trapping and diatomic subradiance on the fluorescence decay, depends not only on the size, but also on the frequency of the exciting light. The closer the frequency is to ω_0 , the more efficiently the diffuse mode is excited, the smaller is τ_r ,

and the less the relative role of diatomic clusters. This is well illustrated in Fig. 3, computed with $b_0 \approx 19$ corresponding to $\tau_{\text{diff}} \approx 36\tau_{\text{at}}$ (neglecting the extrapolation length): As the detuning δ increases, the time to reach the stationary decay rate (due to radiation trapping) also increases. The curves also show a tendency to reach an intermediate stationary value due to diatomic clusters, in the range around $\gamma t \sim 50$, which is more pronounced at large detuning (see the curve corresponding to $\delta = -5\gamma$).

In the following subsections we present further arguments in favor of a diffusive interpretation of the slow decay at late time, by looking at other observables, namely the spatial distribution of excitation, the spectrum and the polarization of the fluorescence.

B. Spatial distribution of excitation

From the CD model we can analyze the spatial distribution of the excitation, which is encoded in $|b_e|^2$, and its change with time. This distribution is shown in Fig. 4 for two time delays after the end of the pulse.

At some intermediate stage of the slow fluorescence decay ($\gamma t = 30$, Fig. 4, upper panel), the distribution of atomic excitation is practically homogeneous on average, although it exhibits relatively strong fluctuations, due to the limited number (300) of ensembles used for averaging, and the relatively small number of pairs. When these excited states decay, the main contribution begins to be made by the longer-lived diffusion mode, whose shape can be computed from the diffusion equation: It is characterized by one half sine distribution over the ensemble ($\gamma t = 180$, Fig. 4, lower panel). At the boundaries of the cloud, the excitation is not zero. It vanishes at some distance on the order of the mean free-path from the boundary of the cloud (extrapolation length). That is why the time τ_r (Eq. 5) is determined not by the optical thickness b_0 , but by a slightly larger value b . Until the slowest diffusion mode decays, the distribution form does not change, only the absolute value of the excitation density decreases. There are also some localized spikes that correspond to excited diatomic clusters.

The transition from long-lived extended modes to longer-lived diffusive modes is consistent with the analysis of Ref. [40], in which the relative population of the collective modes has been studied as a function of the detuning of the driving field. It has been shown that the diffusive modes are very weakly populated when the system is driven out of resonance. That's why they are visible only after a long decay time, with correspondingly a very low relative fluorescence intensity. Note that the spatial profile of the driving beam has also an impact on which modes are preferentially populated [38].

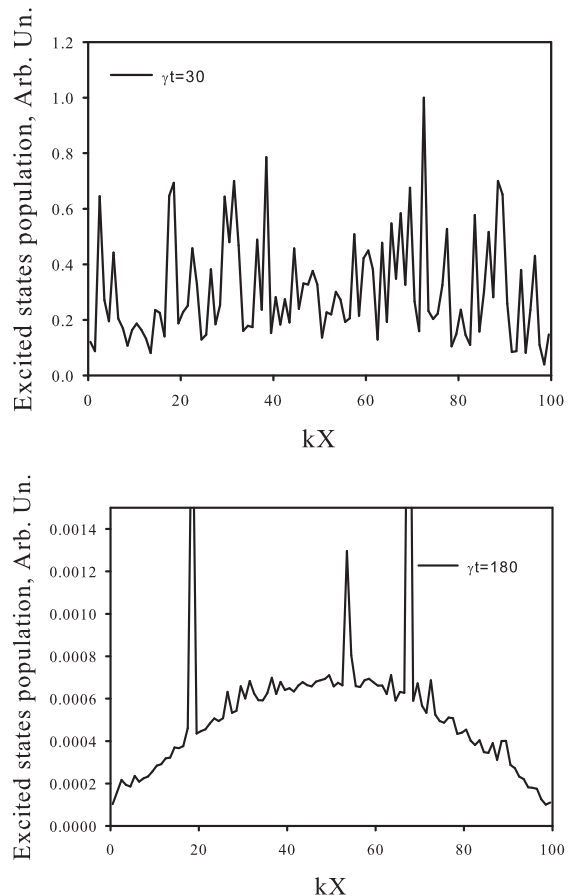


FIG. 4. Cut of the spatial distribution of excited atoms for two time delays after the switch-off of the excitation, $\gamma t = 30$ (top) and $\gamma t = 180$ (bottom). The parameters are $kL = 100$, $\delta = -4\gamma$ and the number of realizations is 300. The width of the cut is $0.5/k$.

C. Fluorescence spectrum

The change of the decay mechanism with time can also be verified by analyzing the spectrum of the secondary radiation, which is determined by a short-term Fourier transform [41] with a rectangular window of duration $\gamma\Delta t = 30$.

The upper panel of Fig. 5 shows the spectrum of the radiation scattered at an angle $\theta = \pi/4$ for the case when the middle of the time window corresponds to $\gamma t = 20$ after the end of the excitation. At this stage, we observe a Lorentzian line at the excitation frequency $\delta = -4\gamma$, as well as a distorted broad line near the free-atom resonance. This shape of the spectrum shows that the non-resonant driving field effectively excites diatomic quasi-molecules, which are relatively few in a dilute medium, and with a low probability excites numerous collective states with frequencies close to the transition frequency of free atoms.

At later time the relative contribution of radiation

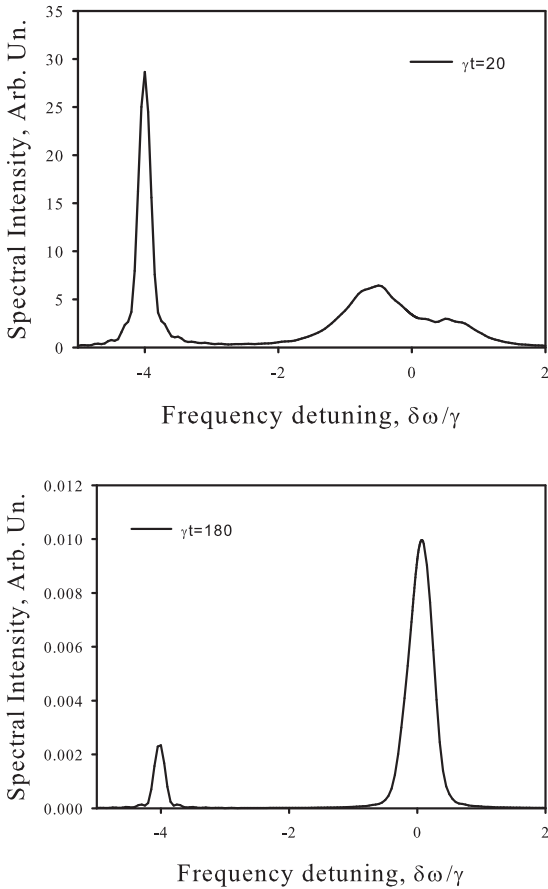


FIG. 5. Fluorescence spectrum for two time delays after the switch-off of the excitation, $\gamma t = 20$ (top) and $\gamma t = 180$ (bottom). The parameters are $kL = 100$ and $\delta = -4\gamma$.

at the excitation frequency decreases ($\gamma t = 180$, Fig. 5, lower panel). The main contribution to the radiation then comes from the collective states unshifted in frequency. This shows that at late time, the emitted radiation is mainly at the atomic resonance and thus can undergo multiple scattering in the optically-thick medium.

D. Fluorescence polarization

Another interesting property of the slow-decaying fluorescence is its polarization. In Fig. 6 we show the time-dependence of the decaying intensities in two orthogonal polarization channels. We observe that at very short time, during the superradiant decay, light is polarized, which is consistent with a single-scattering interpretation of superradiance, such as the one given in [42]. Then when multiple scattering starts to occur, the degree of polarization decreases. At intermediate time though, light remains partially polarized, which is consistent with radiation by diatomic clusters. Finally, at later time ($\gamma t \gtrsim 150$), light is completely depolarized, with equal

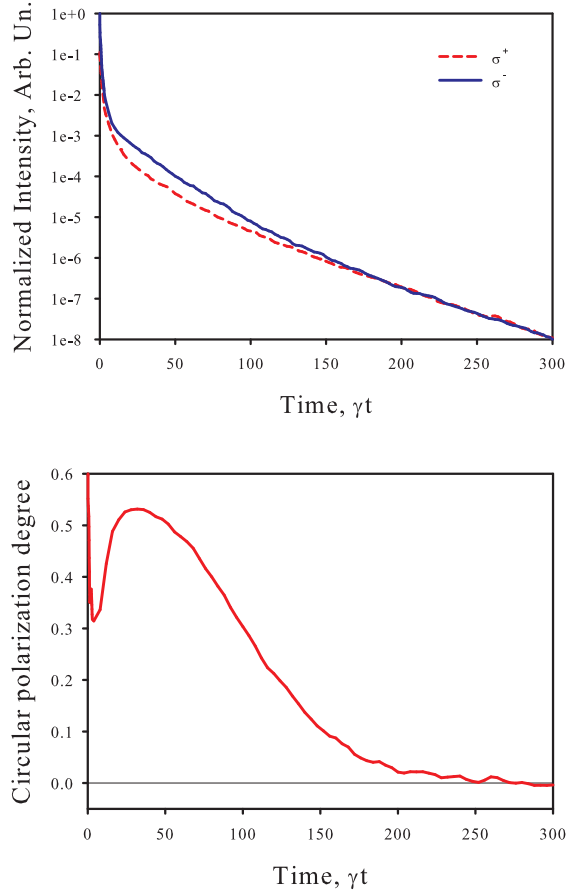


FIG. 6. Upper panel: Normalized intensities of two orthogonal circularly polarized components of the radiation emitted at an angle $\theta = \pi/4$. The incident radiation is left circularly polarized and the other parameters are $kL = 100$ and $\delta = -4\gamma$. Lower panel: Corresponding degree of circular polarization.

intensities in the two polarization channels, which is well consistent with multiply-scattered light. This observation, also reported in [43], supports the interpretation that late-time subradiance is due to radiation trapping.

IV. DISCUSSION AND CONCLUSION

One clear signature of a diffusive behavior is the quadratic scaling of Eq.(5): the lifetime associated to radiation trapping increases quadratically with the system size (or b_0). In the framework of the CD model, this quadratic dependence of slow-decaying modes has not been reported so far. On the contrary, linear scaling of the subradiant lifetime has been observed in [4, 5, 36, 38, 43, 44]. This might be due to the computational limitations of the CD model: reaching large-enough b_0 to reach the diffusive regime without introducing high-density effects [43] needs atom numbers that are

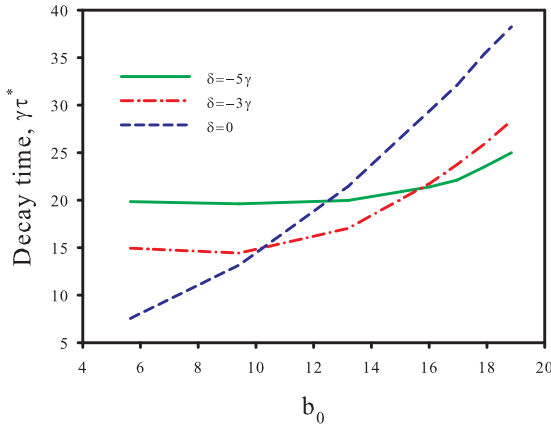


FIG. 7. Dependence of the characteristic decay time τ^* with the resonant optical thickness for different detuning δ of the driving field.

out of reach, or at least very difficult to handle. Another constraint is the time it takes to reach the slowest decay rate (see Fig. 3), which imposes to measure the decay rate at very late time and subsequently at very low relative intensity level, out of reach experimentally.

To illustrate those difficulties we show in Fig. 7 the instant trapping time τ^* when the fluorescence intensity is 10^{-6} from the initial one, as a function of b_0 , up to $b_0 \approx 19$ ($N = 10000$). For detuned excitation, there is a range of b_0 for which the decay time remains practically constant. This constant value increases with the detuning. In this range of parameters, the dominant contribution to the fluorescence is made by diatomic clusters. The characteristic decay time here is determined by the lifetime of the excited states of those quasimolecules, the transition frequency of which coincides with the frequency of the driving field. At larger optical depth, the effect of radiation trapping is visible and the decay time increases. However, we don't reach the regime where a quadratic scaling would be well visible. Note that in experiments, atomic motion also breaks the quadratic dependence of the radiation trapping lifetime because of the Doppler-induced frequency redistribution [19, 45, 46].

Atomic motion also probably strongly reduces the in-

fluence of diatomic clusters, which was the reason to neglect them in previous works [5, 36, 38, 43]. Indeed, experimental results never exhibit lifetimes that are independent of b_0 , as shown in Fig. 1. This should be confirmed by further numerical studies using moving atoms [44, 47]. Note that, in addition to thermal motion, pairs are also affected by the attractive force induced by the near-field interaction and the subsequent inelastic collision and light emission [48, 49].

Furthermore, we stress that the quadratic scaling is predicted using a diffusion approach, which practically neglects all wave effects. It is thus a crude approximation. Therefore it cannot be excluded that the richer physics included in the CD model and in experiments change the behavior of the long-lived modes. This could be tested by a careful comparison between the results provided by the CD model and by a random walk model, as previously used for describing radiation trapping [19, 38, 45, 46, 50]. However, the two models have different computational limitations such that a direct comparison is challenging for dynamical problems (it has been done for steady-state scattering in [51, 52]). It is thus left for future work.

Finally, we note that the developed numerical methods to study the polarization and spectrum from the CD approach can also be used in other contexts, such as highly sensitive laser polarization-optical analysis of the properties of ensembles of impurities in perfect optical crystals [53].

ACKNOWLEDGMENTS

We thank A. Cipris, P. Weiss and R. Bachelard for fruitful discussions. The work was carried out within the framework of the State Task for Basic Research (topic code FSEG-2020-0024). Part of this work has been performed in the framework of State task 075-01073-20-00 on the topic No. 0074-2019-0007 of the Ministry of Science and Higher Education of the Russian Federation, and other parts in the framework of the European project ANDLICA, ERC Advanced grant No. 832219. We also acknowledge funding from the French National Research Agency (projects PACE-IN ANR19-QUAN-003 and QuaCor ANR19-CE47-0014).

[1] D. E. Chang, J. S. Douglas, A. González-Tudela, C.-L. Hung, and H. J. Kimble, “*Colloquium: Quantum matter built from nanoscopic lattices of atoms and photons*,” Rev. Mod. Phys. **90**, 031002 (2018).

[2] R. H. Dicke, “*Coherence in spontaneous radiation processes*,” Phys. Rev. **93**, 99–110 (1954).

[3] D. Pavolini, A. Crubellier, P. Pillet, L. Cabaret, and S. Liberman, “*Experimental evidence for subradiance*,” Phys. Rev. Lett. **54**, 1917–1920 (1985).

[4] T. Bienaimé, N. Piovella, and R. Kaiser, “*Controlled Dicke subradiance from a large cloud of two-level systems*,” Phys. Rev. Lett. **108**, 123602 (2012).

[5] W. Guerin, M. O. Araújo, and R. Kaiser, “*Subradiance in a large cloud of cold atoms*,” Phys. Rev. Lett. **116**, 083601 (2016).

[6] S. D. Jenkins, J. Ruostekoski, N. Papasimakis, S. Savo, and N. I. Zheludev, “*Many-body subradiant excitations in metamaterial arrays: Experiment and theory*,” Phys. Rev. Lett. **119**, 053901 (2017).

[7] P. Solano, P. Barberis-Blostein, F. K. Fatemi, L. A. Orozco, and S. L. Rolston, “Super-radiance reveals infinite-range dipole interactions through a nanofiber,” *Nature Comm.* **8**, 1857 (2017).

[8] J. Rui, D. Wei, A. Rubio-Abadal, S. Hollerith, J. Zeiher, D. M. Stamper-Kurn, C. Gross, and I. Bloch, “A subradiant optical mirror formed by a single structured atomic layer,” *Nature* **583**, 369–375 (2020).

[9] M. O. Scully, “Single photon subradiance: Quantum control of spontaneous emission and ultrafast readout,” *Phys. Rev. Lett.* **115**, 243602 (2015).

[10] G. Facchinetto, S. D. Jenkins, and J. Ruostekoski, “Storing light with subradiant correlations in arrays of atoms,” *Phys. Rev. Lett.* **117**, 243601 (2016).

[11] H. H. Jen, M.-S. Chang, and Y.-C. Chen, “Cooperative single-photon subradiant states,” *Phys. Rev. A* **94**, 013803 (2016).

[12] A. Asenjo-Garcia, M. Moreno-Cardero, A. Albrecht, H. J. Kimble, and D. E. Chang, “Exponential improvement in photon storage fidelities using subradiance and “selective radiance” in atomic arrays,” *Phys. Rev. X* **7**, 031024 (2017).

[13] R. Holzinger, D. Plankensteiner, L. Ostermann, and H. Ritsch, “Nanoscale coherent light source,” *Phys. Rev. Lett.* **124**, 253603 (2020).

[14] A. A. Svidzinsky and J.-T. Chang, “Cooperative spontaneous emission as a many-body eigenvalue problem,” *Phys. Rev. A* **77**, 043833 (2008).

[15] A. A. Svidzinsky, J.-T. Chang, and M. O. Scully, “Cooperative spontaneous emission of N atoms: Many-body eigenstates, the effect of virtual Lamb shift processes, and analogy with radiation of N classical oscillators,” *Phys. Rev. A* **81**, 053821 (2010).

[16] W. Guerin, M. T. Rouabah, and R. Kaiser, “Light interacting with atomic ensembles: collective, cooperative and mesoscopic effects,” *J. Mod. Opt.* **64**, 895–907 (2017).

[17] N. J. Schilder, C. Sauvan, J.-P. Hugonin, S. Jennewein, Y. R. P. Sortais, A. Browaeys, and J.-J. Greffet, “Role of polaritonic modes on light scattering from a dense cloud of atoms,” *Phys. Rev. A* **93**, 063835 (2016).

[18] F. Cottier, R. Kaiser, and R. Bachelard, “Role of disorder in super- and subradiance of cold atomic clouds,” *Phys. Rev. A* **98**, 013622 (2018).

[19] G. Labeyrie, E. Vaujour, C. A. Müller, D. Delande, C. Miniatura, D. Wilkowski, and R. Kaiser, “Slow diffusion of light in a cold atomic cloud,” *Phys. Rev. Lett.* **91**, 223904 (2003).

[20] M. C. W. van Rossum and Th. M. Nieuwenhuizen, “Multiple scattering of classical waves: microscopy, mesoscopy, and diffusion,” *Rev. Mod. Phys.* **71**, 313–371 (1999).

[21] L. L. Foldy, “The multiple scattering of waves. I. General theory of isotropic scattering by randomly distributed scatterers,” *Phys. Rev.* **67**, 107–119 (1945).

[22] M. Lax, “Multiple scattering of waves,” *Rev. Mod. Phys.* **23**, 287–310 (1951).

[23] J. Javanainen, J. Ruostekoski, B. Vestergaard, and M. R. Francis, “One-dimensional modeling of light propagation in dense and degenerate samples,” *Phys. Rev. A* **59**, 649–666 (1999).

[24] M. Rusek, J. Mostowski, and A. Orlowski, “Random green matrices: From proximity resonances to Anderson localization,” *Phys. Rev. A* **61**, 022704 (2000).

[25] F. A. Pinheiro, M. Rusek, A. Orlowski, and B. A. van Tiggelen, “Probing Anderson localization of light via decay rate statistics,” *Phys. Rev. E* **69**, 026605 (2004).

[26] H. Fu and P. R. Berman, “Microscopic theory of spontaneous decay in a dielectric,” *Phys. Rev. A* **72**, 022104 (2005).

[27] Ph. W. Courteille, S. Bux, E. Lucioni, K. Lauber, T. Biénaimé, R. Kaiser, and N. Piovella, “Modification of radiation pressure due to cooperative scattering of light,” *Eur. Phys. J. D.* **58**, 69–73 (2010).

[28] D. V. Kuznetsov, Vl. K. Roerich, and M. G. Gladush, “Local field and radiative relaxation rate in a dielectric medium,” *JETP* **113**, 647–658 (2011).

[29] S. E. Skipetrov and I. M. Sokolov, “Absence of Anderson localization of light in a random ensemble of point scatterers,” *Phys. Rev. Lett.* **112**, 023905 (2014).

[30] L. Bellando, A. Gero, E. Akkermans, and R. Kaiser, “Cooperative effects and disorder: A scaling analysis of the spectrum of the effective atomic Hamiltonian,” *Phys. Rev. A* **90**, 063822 (2014).

[31] S. E. Skipetrov and I. M. Sokolov, “Magnetic-field-driven localization of light in a cold-atom gas,” *Phys. Rev. Lett.* **114**, 053902 (2015).

[32] A. S. Kuraptsev and I. M. Sokolov, “Reflection of resonant light from a plane surface of an ensemble of motionless point scatters: Quantum microscopic approach,” *Phys. Rev. A* **91**, 053822 (2015).

[33] M. O. Araújo, I. Krešić, R. Kaiser, and W. Guerin, “Superradiance in a large cloud of cold atoms in the linear-optics regime,” *Phys. Rev. Lett.* **117**, 073002 (2016).

[34] I.M. Sokolov, D.V. Kupriyanov, and M.D. Havey, “Microscopic theory of scattering of weak electromagnetic radiation by a dense ensemble of ultracold atoms,” *JETP* **112**, 246 (2011).

[35] A. S. Kuraptsev, I. Sokolov, and M. D. Havey, “Angular distribution of single photon superradiance in a dilute and cold atomic ensemble,” *Phys. Rev. A* **96**, 023830 (2017).

[36] M. O. Araújo, W. Guerin, and R. Kaiser, “Decay dynamics in the coupled-dipole model,” *J. Mod. Opt.* **65**, 1345–1354 (2018).

[37] A. Gero and E. Akkermans, “Effect of superradiance on transport of diffusing photons in cold atomic gases,” *Phys. Rev. Lett.* **96**, 093601 (2006).

[38] P. Weiss, M. O. Araújo, R. Kaiser, and W. Guerin, “Subradiance and radiation trapping in cold atoms,” *New. J. Phys.* **20**, 063024 (2018).

[39] H. Cao, “Lasing in random media,” *Waves Random Media* **13**, R1–R39 (2003).

[40] W. Guerin and R. Kaiser, “Population of collective modes in light scattering by many atoms,” *Phys. Rev. A* **95**, 053865 (2017).

[41] S. V. Bozhokin and I. M. Sokolov, “Comparison of the wavelet and Gabor transforms in the spectral analysis of nonstationary signals,” *Tech. Phys.* **63**, 1711–1717 (2018).

[42] P. Weiss, A. Cipris, R. Kaiser, I. M. Sokolov, and W. Guerin, “Superradiance as single scattering embedded in an effective medium,” *arXiv:2011.05201*.

[43] A. Cipris, R. Bachelard, R. Kaiser, and W. Guerin, “Van der Waals dephasing for Dicke subradiance in cold atomic clouds,” (2021), *arXiv:2012.06248*.

[44] P. Weiss, A. Cipris, M. O. Araújo, R. Kaiser, and W. Guerin, “Robustness of Dicke subradiance against

thermal decoherence,” *Phys. Rev. A* **100**, 033833 (2019).

[45] G. Labeyrie, R. Kaiser, and D. Delande, “Radiation trapping in a cold atomic gas,” *Appl. Phys. B* **81**, 1001–1008 (2005).

[46] R. Pierrat, B. Grémaud, and D. Delande, “Enhancement of radiation trapping for quasiresonant scatterers at low temperature,” *Phys. Rev. A* **80**, 013831 (2009).

[47] A. S. Kuraptsev and I. M. Sokolov, “Influence of atomic motion on the collective effects in dense and cold atomic ensembles,” *Phys. Rev. A* **101**, 033602 (2020).

[48] A. R. L. Caires, G. D. Telles, M. W. Mancini, L. G. Marcella, V. S. Bagnato, D. Wilkowski, and R. Kaiser, “Intensity dependence for trap loss rate in a magneto-optical trap of strontium,” *Braz. J. Phys.* **34**, 1504 (2004).

[49] A. Fuhrmanek, R. Bourgain, Y. R. P. Sortais, and A. Browaeys, “Light-assisted collisions between a few cold atoms in a microscopic dipole trap,” *Phys. Rev. A* **85**, 062708 (2012).

[50] V. M. Datsyuk and I. M. Sokolov, “Coherent backscattering under conditions of pulsed radiation trapping,” *JETP* **102**, 724–736 (2006).

[51] J. Chabé, M. T. Rouabah, L. Bellando, T. Bienaimé, N. Piovella, R. Bachelard, and R. Kaiser, “Coherent and incoherent multiple scattering,” *Phys. Rev. A* **89**, 043833 (2014).

[52] I. M. Sokolov and W. Guerin, “Comparison of three approaches to light scattering by dilute cold atomic ensembles,” *J. Opt. Soc. Am. B* **36**, 2030–3037 (2019).

[53] Y.A. Fofanov, V.V. Manoylov, I.V. Zarutskiy, and Kuraptsev A.S, “Laser polarization-optical diagnostics of ordered objects and structures,” *Bull. Russ. Acad. Sci. Phys.* **84**, 263–266 (2020).